

Original Article



OPEN ACCESS

Received: Feb 19, 2018

Revised: May 11, 2018

Accepted: Jun 5, 2018

Correspondence to

Dong Seok Lee, MD, PhD

Department of Pediatrics, Dongguk University
School of Medicine, 87, Dongdae-ro,
Gyeongju 38067, Korea.
E-mail: lds117@dongguk.ac.kr

Copyright © 2018. The Korean Society of
Cardiology

This is an Open Access article distributed
under the terms of the Creative Commons
Attribution Non-Commercial License ([https://
creativecommons.org/licenses/by-nc/4.0](https://creativecommons.org/licenses/by-nc/4.0))
which permits unrestricted noncommercial
use, distribution, and reproduction in any
medium, provided the original work is properly
cited.

ORCID iDs

Dong Seok Lee

<https://orcid.org/0000-0001-9542-8250>

Yong Wook Jung

<https://orcid.org/0000-0001-7285-4521>

Funding

This work was financially supported by the
grant of The Korean Society of Circulation in
2011 and the research fund from Dongguk
University.

Conflict of Interest

The authors have no financial conflicts of
interest.

Protective Effect of Right Ventricular Mitochondrial Damage by Cyclosporine A in Monocrotaline-induced Pulmonary Hypertension

Dong Seok Lee , MD, PhD¹, and Yong Wook Jung , MD, PhD²

¹Department of Pediatrics, Dongguk University School of Medicine, Gyeongju, Korea

²Department of Anatomy, Dongguk University School of Medicine, Gyeongju, Korea

ABSTRACT

Background and Objectives: Mitochondria play a key role in the pathophysiology of heart failure and mitochondrial permeability transition pore (MPTP) play a critical role in cell death and a critical target for cardioprotection. The aim of this study was to evaluate the protective effects of cyclosporine A (CsA), one of MPTP blockers, and morphological changes of mitochondria and MPTP related proteins in monocrotaline (MCT) induced pulmonary arterial hypertension (PAH).

Methods: Eight weeks old Sprague-Dawley rats were randomized to control, MCT (60 mg/kg) and MCT plus CsA (10 mg/kg/day) treatment groups. Four weeks later, right ventricular hypertrophy (RVH) and morphological changes of right ventricle (RV) were done. Western blot and reverse transcription polymerase chain reaction (RT-PCR) for MPTP related protein were performed.

Results: In electron microscopy, CsA treatment prevented MCT-induced mitochondrial disruption of RV. RVH was significantly increased in MCT group compared to that of the controls but RVH was more increased with CsA treatment. Thickened medial wall thickness of pulmonary arteriole in PAH was not changed after CsA treatment. In western blot, caspase-3 was significantly increased in MCT group, and was attenuated in CsA treatment. There were no significant differences in voltage-dependent anion channel, adenine nucleotide translocator 1 and cyclophilin D expression in western blot and RT-PCR between the 3 groups.

Conclusions: CsA reduces MCT induced RV mitochondrial damage. Although, MPTP blocking does not reverse pulmonary pathology, it may reduce RV dysfunction in PAH. The results suggest that it could serve as an adjunctive therapy to PAH treatment.

Keywords: Pulmonary circulation; Pulmonary hypertension; Heart ventricles; Mitochondria

INTRODUCTION

Pulmonary arterial hypertension (PAH) is characterized by abnormal proliferation of vascular endothelial and smooth muscle cells, and causes the occlusion of pulmonary arterioles which eventually results in right heart failure (HF) and death.^{1,2)} Until now, the therapeutic target of PAH was focused mostly on vascular abnormality. Although there is no perfect cure for PAH

Author Contributions

Conceptualization: Lee DS; Data curation: Lee DS, Jung YW; Formal analysis: Lee DS; Funding acquisition: Lee DS; Investigation: Jung YW; Methodology: Lee DS; Project administration: Lee DS; Validation: Lee DS; Writing - original draft: Lee DS, Jung YW; Writing - review & editing: Lee DS.

yet, newer medical therapies have been shown to improve survival rate, exercise tolerance, hemodynamics, and quality of life.³⁾ Despite the significance of right HF to survival, there are no therapies that directly or selectively improve right ventricular function.

The right heart has been a direct target of recent PAH treatments, especially the mitochondria which play an essential role in the progression of HF.⁴⁾

Mitochondria are critical mediators of cellular life through energy production as well as cell death through induction of apoptosis and necrosis.⁵⁾ While many death pathways converge on mitochondria, there has been a growing set of evidence indicating that the mitochondrial permeability transition pore (MPTP) is heavily involved in mediating cardiac dysfunction and cell death.⁵⁾ Mitochondrial permeability transition is the phenomenon whereby the inner membrane suddenly allows free passage of solutes up to 1.5 kDa in size.⁶⁾ Prolonged MPTP opening results in inner membrane potential collapse, respiratory chain uncoupling, halt of mitochondrial adenosine-5'-triphosphate (ATP) synthesis, and eventually mitochondrial swelling, rupture, and cell death.⁷⁾ Many studies have shown that MPTP opens during myocardial reperfusion injury due to oxidative stress, Ca²⁺ overload, decreased ATP levels and increased matrix pH, which cause more necrosis and apoptosis of cardiac myocyte.⁸⁾⁹⁾ Inhibiting the opening of MPTP by cyclosporine A (CsA) produces cardioprotection against ischemia reperfusion injury¹⁰⁾¹¹⁾ and post-myocardial infarction HF.¹²⁾

However, the mitochondrial dysfunction in PAH has not been well known. The aim of this study was to evaluate the protective effects of CsA, one of MPTP blockers, and the morphological changes of mitochondria and MPTP related proteins of hypertrophied right ventricle (RV) in monocrotaline (MCT) induced PAH.

METHODS

Experimental design

Eight-week-old male Sprague-Dawley rats weighing 200–220 g were housed under standardized environmental conditions (12 hours light/dark cycle, 21±1°C and 55±5% humidity) with free access to chow and water. PAH was induced by subcutaneous (sc) injection of 60 mg/kg MCT (Sigma-Aldrich, St. Louis, MO, USA). The rats were grouped into a control (NC) group (n=8) that received sc injection of normal saline (0.1 mL/kg); MCT group (n=8) that received sc injection of MCT; and MCTCsA group (n=8) that received sc injection of MCT plus 10 mg/kg/day CsA-containing chow orally (Chong Kun Dang, Pharma, Korea). We chose the dose of 10 mg/kg because this dose of CsA had no biochemical evidence of renal injury or hemodynamic effect.¹¹⁾¹³⁾

The rats were sacrificed after 4 weeks. Heart and lung tissues were removed and dissected, with each sample weighed and frozen in liquid nitrogen. The experimental procedures used were reviewed and approved by the Institutional Animal Care and Use Committee of Dongguk University. Animal care and use were in accordance with the guidelines of the National Institutes of Health (Bethesda, MD, USA).

Right ventricular hypertrophy and total lung weight

The relative cardiac weight of the RV/left ventricle (LV)+septum (RV/LV+S) ratio (i.e., right heart index) was calculated for the assessment of the right ventricular hypertrophy (RVH).

Myocardial fibrilla hypertrophy was measured by NIS-Element AR (version 4.5). Body weight (BW) and total lung weight (TLW) were measured for evaluate the pulmonary congestion. To remove the influence of BW on TLW, we calculated the TLW/BW (100 gm) ratios.

Histologic examination

The rats were perfusion-fixed with 4% paraformaldehyde in 0.1 M phosphate buffer (pH 7.4) under anesthesia. The right lobes of the rat lungs and hearts, including RV, of 8 rats from each group were cut and post-fixed with 4% paraformaldehyde, dehydrated through graded alcohols, and embedded in paraffin wax. The lower zone of the right lung and RV tissue specimens were cut into 5 μ m-thick section and subjected to hematoxylin and eosin staining prior to examination by light microscope. Histopathological study, we measured the thickening of the medial wall of the small intrapulmonary arteries and the size of the cardiomyocytes in the RV.

Transmission electron microscopy

Cross-sections of the ventricular myocardium (approximately 1 mm³) were taken from the RV after fixing in cold 2.5% glutaraldehyde in 0.1 M phosphate-buffered saline (PBS) for 2–4 hours, followed by incubation with 1% osmic acid for 2 hours after rinsing, dehydrated with alcohol, substituted with propylene oxide and embedded in epoxy resin (Epon 812; Sigma-Aldrich). Ultrathin sections (60 nm) were made from the resin-embedded samples and stained with uranyl acetate and lead citrate prior to examination by H-7500 transmission electron microscopy (TEM; Hitachi, Tokyo, Japan).

Subcellular fractionation and immunoblot analysis

The RV tissue was weighed, homogenized using a polytron homogenizer in 1:5 (wt:vol) isotonic HEPES isolation media (20 mM HEPES pH 7.4, 250 mM sucrose, 10 mM KCl, 1.5 mM MgCl₂, 1 mM ethylene glycol tetraacetic acid, 1 mM ethylenediaminetetraacetic acid) supplemented with protease inhibitors, and then centrifuged at 750 \times g for 10 minutes. The resulting supernatant was centrifuged at 14,000 \times g for 10 minutes and the pellet taken as the crude mitochondrial fraction. The remaining supernatant was centrifuged at 100,000 \times g for 60 minutes and the supernatant was taken as the cytosolic fraction. Aliquots were stored at -70°C.

Samples of each fraction were run on 9–15% polyacrylamide minigels (Bio-Rad Mini Protean II; Bio-Rad, Hercules, CA, USA). After electrophoresis, the separated protein was transferred to nitrocellulose membrane in a buffer solution containing 50 mM tris-base, 380 mM glycine and 20% methanol. Membranes were blocked with 5% milk in PBS-T for 1 hour and incubated overnight at 4°C with anti-voltage-dependent anion channel (VDAC) rabbit polyclonal antibody (Santa Cruz Biotechnology, Inc., Santa Cruz, CA, USA), anti-adenine nucleotide translocator 1 (ANT1) goat polyclonal antibody (Santa Cruz Biotechnology, Inc.), rabbit anti-cyclophilin D (CypD) (Santa Cruz Biotechnology, Inc.) using mitochondrial fraction, anti-AIF goat polyclonal antibody (Santa Cruz Biotechnology, Inc.), and anti-caspase-3 (Casp3) rabbit polyclonal antibody (Santa Cruz Biotechnology, Inc.) using cytosolic fraction. The sites of antibody-antigen reaction were visualized with horse radish peroxidase (HRP)-conjugated secondary antibodies (P447 or P448; Dako, Glostrup, Denmark), an enhanced chemiluminescence (ECL; Amersham Pharmacia Biotech, Little Chalfont, UK) system, and exposure to photographic film (Hyperfilm ECL, RPN3103K; Amersham Pharmacia Biotech). The immunoblot signal developed by ECL system was quantified using Scion Image software (version 1.59; National Institutes of Health).

Semi-quantitative reverse transcription polymerase chain reaction

Tissues were rapidly frozen by liquid nitrogen and stored at -80°C . Total RNA in individual heart sample was extracted by easy-BLUE™ Total RNA Extraction kit (iNtRON Biotechnology, Sungnam, Korea) according to the manufacturer's protocol. 1 μg of total RNA was used for cDNA synthesis and PCR amplification; reverse transcription polymerase chain reaction (RT-PCR) was performed with RNA PCR kit (avian myeloblastosis virus) ver. 3.0 (Takara, Shiga, Japan). Primer sequences of VDAC were 5'-GGACCGAGTATGGGCTGACG-3' and 5'-GCTGCTATCCAAAGCGAGTGTTAC-3', ANTI were 5'-TTCCCCACCCAAGCTCTCAACT-3' and 5'-CGGCTGTACACTCTGGGCAATCA-3', CypD were 5'-CTAGGACAGCAGCAGGCAGC-3' and 5'-TTGAGCAGACAGGCCTGGCT-3', GAPDH were 5'-TGAACGGGAAGCTCACTGG-3' and 5'-CCACCACCCTGTTGCTGTA-3'. PCR products were subjected to agarose gel electrophoresis containing 0.5 $\mu\text{g}/\text{mL}$ of ethidium bromide and were observed by an UV transilluminometer. Glyceraldehyde 3-phosphate dehydrogenase (GAPDH) was used as internal control.

Statistical analysis

All data was presented as mean \pm standard deviation (SD). Data was analyzed by 1-way analysis of variance (ANOVA) followed by Tukey's honestly significant different multiple-comparison test. Multiple-comparison tests were only applied when a significant difference was determined by ANOVA. Statistical hypotheses were considered significant if $p < 0.05$.

RESULTS

Changes in right ventricular hypertrophy and myocardial fibrilla hypertrophy

RV mass was significantly increased in MCT group compared to that of the controls (0.29 ± 0.02 vs. 0.51 ± 0.06 , $p = 0.005$), but the RVH was more increased in CsA treatment group (0.51 ± 0.02 vs. 0.57 ± 0.01 , $p = 0.045$). Myocardial fibrilla hypertrophy was significantly increased in MCT group ($340.1 \pm 43.1 \mu\text{m}^2$ vs. $393.8 \pm 44.7 \mu\text{m}^2$, $p = 0.014$). Interestingly, the CsA treatment induced myocardial fibrilla hypertrophy even more ($393.8 \pm 44.7 \mu\text{m}^2$ vs. $489.9 \pm 75.3 \mu\text{m}^2$, $p = 0.000$; **Table 1**).

Pulmonary artery medial wall thickness and total lung weight

MCT treatment increased medial wall thickness (MWT ratio) of pulmonary arteriole compared with that of the control (0.12 ± 0.03 vs. 0.19 ± 0.03 , $p = 0.000$), but CsA treatment did not change MCT induced thickened MWT (0.19 ± 0.03 vs. 0.20 ± 0.04 , $p = 0.308$).

TLW was significantly increased in MCT group compared to that of the control (0.39 ± 0.04 vs. 0.61 ± 0.07 , $p = 0.032$). CsA treatment significantly reduced TLW (0.61 ± 0.07 vs. 0.45 ± 0.03 , $p = 0.009$; **Table 2**).

Table 1. RVH and myocardial fibrilla hypertrophy

| | NC | MCT | MCTCsA |
|---|------------------|--------------------|------------------------------|
| RV/LV+IVS | 0.29 ± 0.02 | $0.51 \pm 0.06^*$ | $0.57 \pm 0.01^{* \dagger}$ |
| Myocardial fibrilla hypertrophy (μm^2) | 340.1 ± 43.1 | $393.8 \pm 44.7^*$ | $489.9 \pm 75.3^{* \dagger}$ |

Values are presented as mean \pm SD.

CsA = cyclosporine A; IVS = interventricular septum; LV = left ventricle; MCT = monocrotaline; NC = normal control; RV = right ventricle; RVH = right ventricular hypertrophy; SD = standard deviation.

* $p < 0.05$ vs. NC group; $\dagger p < 0.05$ vs. MCT group.

Table 2. Pulmonary artery MWT and TLW

| | NC | MCT | MCTCSA |
|-----------------|-----------|------------|--------------|
| MWT ratio | 0.12±0.03 | 0.19±0.03* | 0.20±0.04* |
| TLW/BW (100 gm) | 0.39±0.04 | 0.61±0.07* | 0.45±0.03*·† |

Values are presented as mean±SD.

BW = body weight; CsA = cyclosporine A; MCT = monocrotaline; MWT = medial wall thickness; NC = normal control; SD = standard deviation; TLW = total lung weight.

*p<0.05 vs. NC group; †p<0.05 vs. MCT group.

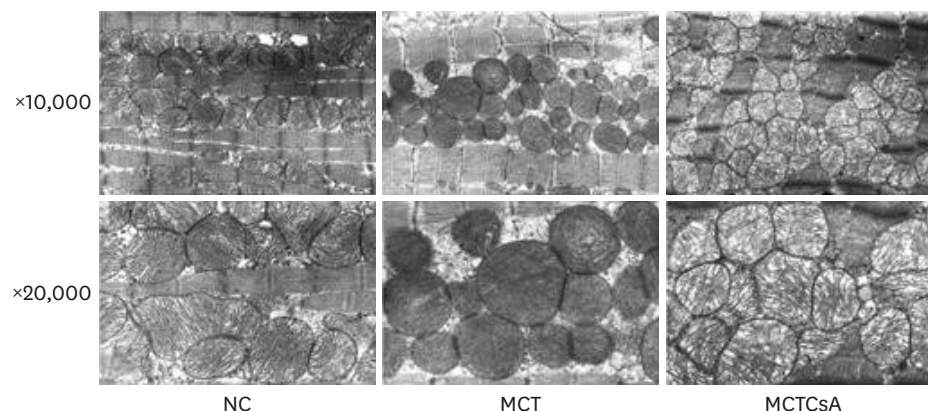


Figure 1. TEM findings. The ultrastructure of the mitochondria in MCT group were swollen, disrupted, and disorganized. CsA treatment prevented mitochondrial damage dramatically (×10,000–20,000). CsA = cyclosporine A; NC = normal control; MCT = monocrotaline; NC = normal control; TEM = transmission electron microscopy.

Transmission electron microscopic changes

In TEM, mitochondria were well defined membranes with tightly packed cristae in normal control group. But, RV mitochondrial damage was significant in MCT induced PAH. The mitochondria of MCT group showed swollen cristae and matrix, loss of integrity, sparse cristae, and membrane disruptions. The CsA treatment prevented such disruptions significantly, but not as intact as the normal control group (**Figure 1**).

Western blotting

In western blot, expression of MPTP proteins, VDAC, ANT1, and CypD were not significantly changed in MCT group and CsA treatment. Casp3 was significantly increased in MCT group (p=0.009), and attenuated in CsA treatment significantly (p=0.027). AIF was slightly increased in MCT group and decreased with CsA treatment, but the difference was not statistically significant (**Figure 2**).

Reverse transcription polymerase chain reaction

In RT-PCR, the expression of VDAC, ANT1, and CypD were unchanged in all 3 groups (**Figure 3**).

DISCUSSION

This study demonstrates that the RV mitochondrial damage is prominent in MCT-induced PAH and that CsA, one of MPTP blockers, prevents MCT-induced mitochondrial damage significantly. In addition, CsA is an important factor to prevent MCT-induced myocardial

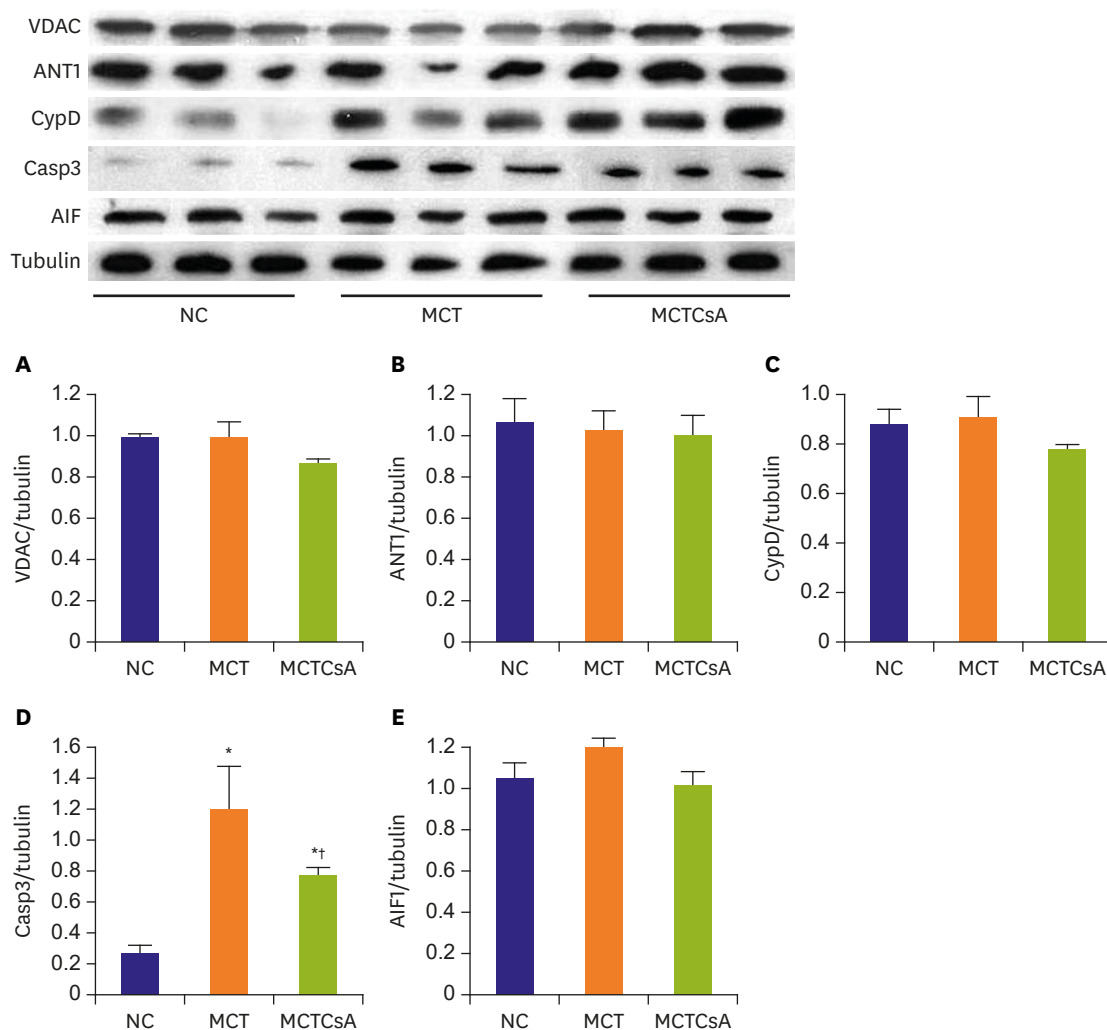


Figure 2. Western blot. There were no significant changes in VDAC, ANTI1, CypD, and AIF expression (A-C and E). Casp3 was significantly increased in MCT group, but was significantly attenuated in CsA treatment (D). Values are presented as mean±SD. AIF = apoptosis-inducing factor; ANTI1 = adenine nucleotide translocator 1; Casp3 = caspase-3; CsA = cyclosporine A; CypD = cyclophilin D; MCT = monocrotaline; NC = normal control; SD = standard deviation; VDAC = voltage-dependent anion channel. *p<0.05 vs. NC group; †p<0.05 vs. MCT group.

damage of PAH by reducing Casp3 expressions. But the expression of molecular components of MPTP (VDAC, ANTI1, and CypD) was not changed.

PAH is characterized by increased pulmonary arterial pressure, resulting in increased RV afterload and subsequent right ventricular failure (RVF). Although recent studies revealed that many other factors are involved, and that the pulmonary artery pressure is not the only cause of RVF,¹⁴⁾ most PAH therapies focus on the regression of pulmonary vascular disease. The prevention or reduction of RVF, together with a pulmonary artery pressure control, may be a new therapeutic strategy for the treatment of PAH.

HF is a multifactorial syndrome, and recent studies revealed that it is largely associated with mitochondrial dysfunction.⁴⁾ Mitochondria act as ATP producers and play a key role in the pathophysiology of HF.⁴⁾ But the mitochondrial dysfunction in PAH remains not well known.

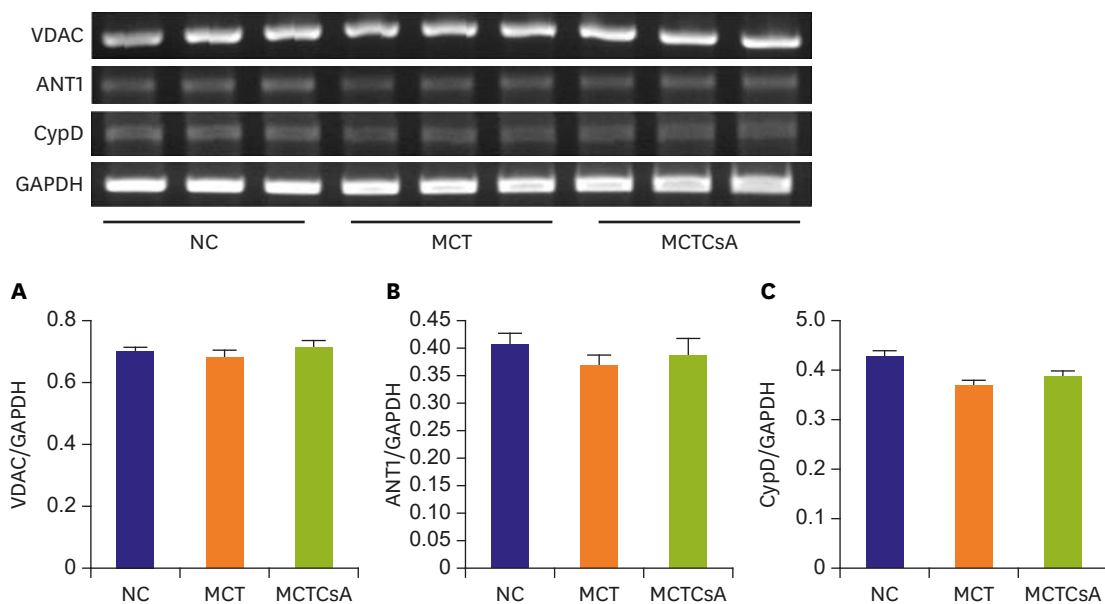


Figure 3. RT-PCR. The expression of VDAC, ANTI, and CypD was not significantly changed in all 3 groups (A-C). Values are presented as mean±SD. ANTI = adenine nucleotide translocator 1; CypD = cyclophilin D; GAPDH = glyceraldehyde-3-phosphate dehydrogenase; MCT = monocrotaline; NC = normal control; RT-PCR = reverse transcription polymerase chain reaction; SD = standard deviation; VDAC = voltage-dependent anion channel.

In an animal model of RVF, the mitochondrial oxygen consumption rate of the RV muscle was decreased, which is associated with a reduction in myocardial high-energy phosphates and decrease in mitochondrial oxygen consumption rate. These results suggest that impairment of the mitochondrial energy-producing ability is involved in the development of the RVF in MCT-induced pulmonary hypertensive rats.¹⁵⁾

In addition to their central role in ATP synthesis, mitochondria also play a critical role in cell death. Especially MPTP in mitochondria acts as a key nodal point in mediating cardiac dysfunction and cell death.⁵⁾⁷⁾ MPTP is comprised of the VDAC in the outer mitochondrial membrane, the ANT in the inner mitochondrial membrane, and CypD as its regulator in the matrix of the mitochondria.⁸⁾ The expression of key molecular of MPTP, VDAC, ANTI, and CypD, remained unchanged throughout this study. This suggests that such molecular function through conformational, rather than quantitative changes. Oxidative stress followed by calcium overload, ATP depletion, and elevated phosphate levels induce MPTP opening.⁸⁾ MPTP opening results in eventual mitochondrial swelling, rupture, and cell death.⁷⁾

It is well known that lung tissue apoptosis plays a key role in the development of PAH.¹⁶⁾ Recently, several studies reported that right ventricular myocardial apoptosis plays a central role in RVF.¹⁷⁾¹⁹⁾ Zungu-Edmondson et al.¹⁹⁾ revealed that apoptosis is observed in early stage of RVF and declined serially in end stage of RVF. These studies provide a new insight of apoptosis to reverse RV failure in PAH. In mitochondria, MPTP opening leads to the release of pro-apoptotic protein cytochrome c (CytC) from the mitochondria into the cytoplasm. The released CytC causes activation of caspase-9, which in turn activates Casp3 leading to apoptosis.²⁰⁾ AIF, also a death-inducing factor independent of caspase, is released into cytoplasm causing apoptosis. In this study, increased Casp3 was suppressed with CsA treatment without significant changes in AIF. This suggests that the main apoptotic pathway of MCT-induced RVF is related with the activation of caspase dependent pathway.²¹⁾

More recent studies showed that MPTP opening plays a crucial role in reperfusion injury.²²⁾ Thus, the MPTP is an attractive target for prevention of cell death in several diseases. Indeed, MPTP inhibition via targeting CypD, recognized as a key molecular component of the MPTP, protects mice from cell death in response to select disease stimuli.²³⁾²⁴⁾

CsA is an inhibitor of MPTP opening by preventing the binding of CypD to the ANT. Some previous animal studies indicated that CsA might reduce myocardial infarct size.²⁵⁾ It also has been proposed to prevent reperfusion injury following acute myocardial infarction.²⁶⁾ However, the effects of CsA in clinical patients remain largely unknown. A small pilot trial showed that administration of CsA at the time of percutaneous coronary intervention limited infarct size during acute myocardial infarction, suggesting a positive effect of CsA in reperfusion injury.²⁷⁾ However, another study with a similar number of patients reported that CsA treatment did not produce any beneficial effects on either infarct size or other clinical outcomes.²⁸⁾

In this study, CsA did not affect medial wall thickness of small pulmonary arterioles and RVH in MCT-induced PAH. It means that CsA may not reduce pulmonary artery pressure. However, the TLW was significantly reduced by CsA treatment. This may be due to decreased congestion of MCT lung, but further evaluation is needed in order to clarify the causality. RVH and myofibrillar hypertrophy were rather increased after CsA therapy, which is believed to be a compensatory hypertrophy to overcome high pulmonary artery pressure.

In electron microscopy, RV mitochondrial damage was prominent in PAH. However, CsA reduced mitochondrial damage significantly. It is expected that the CsA treatment prevents RV damage from MCT-induced PAH by eventually blocking the MPTP opening.

As mentioned above, there are remaining debates on the therapeutic effects of CsA in MI or ischemic disease. Nonetheless, the addition of a target therapy to RV, such as CsA, to conventional treatments is expected to be a new therapeutic strategy in the treatment of PAH.

REFERENCES

1. Humbert M, Morrell NW, Archer SL, et al. Cellular and molecular pathobiology of pulmonary arterial hypertension. *J Am Coll Cardiol* 2004;43:13S-24S.
[PUBMED](#) | [CROSSREF](#)
2. Martin KB, Klinger JR, Rounds SI. Pulmonary arterial hypertension: new insights and new hope. *Respirology* 2006;11:6-17.
[PUBMED](#) | [CROSSREF](#)
3. Lee SH, Rubin LJ. Current treatment strategies for pulmonary arterial hypertension. *J Intern Med* 2005;258:199-215.
[PUBMED](#) | [CROSSREF](#)
4. Rosca MG, Hoppel CL. Mitochondrial dysfunction in heart failure. *Heart Fail Rev* 2013;18:607-22.
[PUBMED](#) | [CROSSREF](#)
5. Kwong JQ, Molkentin JD. Physiological and pathological roles of the mitochondrial permeability transition pore in the heart. *Cell Metab* 2015;21:206-14.
[PUBMED](#) | [CROSSREF](#)
6. Haworth RA, Hunter DR. The Ca²⁺-induced membrane transition in mitochondria. II. Nature of the Ca²⁺ trigger site. *Arch Biochem Biophys* 1979;195:460-7.
[PUBMED](#) | [CROSSREF](#)
7. Halestrap AP. What is the mitochondrial permeability transition pore? *J Mol Cell Cardiol* 2009;46:821-31.
[PUBMED](#) | [CROSSREF](#)

8. Crompton M, Costi A. Kinetic evidence for a heart mitochondrial pore activated by Ca²⁺, inorganic phosphate and oxidative stress. A potential mechanism for mitochondrial dysfunction during cellular Ca²⁺ overload. *Eur J Biochem* 1988;178:489-501.
[PUBMED](#) | [CROSSREF](#)
9. Griffiths EJ, Halestrap AP. Mitochondrial non-specific pores remain closed during cardiac ischaemia, but open upon reperfusion. *Biochem J* 1995;307:93-8.
[PUBMED](#) | [CROSSREF](#)
10. Sheu JJ, Chua S, Sun CK, et al. Intra-coronary administration of cyclosporine limits infarct size, attenuates remodeling and preserves left ventricular function in porcine acute anterior infarction. *Int J Cardiol* 2011;147:79-87.
[PUBMED](#) | [CROSSREF](#)
11. Hausenloy DJ, Boston-Griffiths EA, Yellon DM. Cyclosporin A and cardioprotection: from investigative tool to therapeutic agent. *Br J Pharmacol* 2012;165:1235-45.
[PUBMED](#) | [CROSSREF](#)
12. Lim SY, Hausenloy DJ, Arjun S, et al. Mitochondrial cyclophilin-D as a potential therapeutic target for post-myocardial infarction heart failure. *J Cell Mol Med* 2011;15:2443-51.
[PUBMED](#) | [CROSSREF](#)
13. Bach PH, Lock EA. *Nephrotoxicity: In Vitro and in Vivo, Animals to Man*. 1st ed. New York (NY): Springer Science and Business Media; 2013. p.707.
14. Voelkel NF, Natarajan R, Drake JL, Bogaard HJ. Right ventricle in pulmonary hypertension. *Compr Physiol* 2011;1:525-40.
[PUBMED](#) | [CROSSREF](#)
15. Daicho T, Yagi T, Abe Y, et al. Possible involvement of mitochondrial energy-producing ability in the development of right ventricular failure in monocrotaline-induced pulmonary hypertensive rats. *J Pharmacol Sci* 2009;111:33-43.
[PUBMED](#) | [CROSSREF](#)
16. Hong YM, Kwon JH, Choi S, Kim KC. Apoptosis and inflammation associated gene expressions in monocrotaline-induced pulmonary hypertensive rats after bosentan treatment. *Korean Circ J* 2014;44:97-104.
[PUBMED](#) | [CROSSREF](#)
17. Campian ME, Verberne HJ, Hardziyenka M, et al. Serial noninvasive assessment of apoptosis during right ventricular disease progression in rats. *J Nucl Med* 2009;50:1371-7.
[PUBMED](#) | [CROSSREF](#)
18. Zuo XR, Wang Q, Cao Q, et al. Nicorandil prevents right ventricular remodeling by inhibiting apoptosis and lowering pressure overload in rats with pulmonary arterial hypertension. *PLoS One* 2012;7:e44485.
[PUBMED](#) | [CROSSREF](#)
19. Zungu-Edmondson M, Shults NV, Wong CM, Suzuki YJ. Modulators of right ventricular apoptosis and contractility in a rat model of pulmonary hypertension. *Cardiovasc Res* 2016;110:30-9.
[PUBMED](#) | [CROSSREF](#)
20. Kinnally KW, Peixoto PM, Ryu SY, Dejean LM. Is mPTP the gatekeeper for necrosis, apoptosis, or both? *Biochim Biophys Acta* 2011;1813:616-22.
[PUBMED](#) | [CROSSREF](#)
21. Cregan SP, Dawson VL, Slack RS. Role of AIF in caspase-dependent and caspase-independent cell death. *Oncogene* 2004;23:2785-96.
[PUBMED](#) | [CROSSREF](#)
22. Halestrap AP, Richardson AP. The mitochondrial permeability transition: a current perspective on its identity and role in ischaemia/reperfusion injury. *J Mol Cell Cardiol* 2015;78:129-41.
[PUBMED](#) | [CROSSREF](#)
23. Baines CP, Kaiser RA, Purcell NH, et al. Loss of cyclophilin D reveals a critical role for mitochondrial permeability transition in cell death. *Nature* 2005;434:658-62.
[PUBMED](#) | [CROSSREF](#)
24. Ramachandran A, Lebofsky M, Baines CP, Lemasters JJ, Jaeschke H. Cyclophilin D deficiency protects against acetaminophen-induced oxidant stress and liver injury. *Free Radic Res* 2011;45:156-64.
[PUBMED](#) | [CROSSREF](#)
25. Lim WY, Messow CM, Berry C. Cyclosporin variably and inconsistently reduces infarct size in experimental models of reperfused myocardial infarction: a systematic review and meta-analysis. *Br J Pharmacol* 2012;165:2034-43.
[PUBMED](#) | [CROSSREF](#)
26. Gomez L, Li B, Mewton N, et al. Inhibition of mitochondrial permeability transition pore opening: translation to patients. *Cardiovasc Res* 2009;83:226-33.
[PUBMED](#) | [CROSSREF](#)

27. Piot C, Croisille P, Staat P, et al. Effect of cyclosporine on reperfusion injury in acute myocardial infarction. *N Engl J Med* 2008;359:473-81.
[PUBMED](#) | [CROSSREF](#)
28. Ghaffari S, Kazemi B, Toluey M, Sepehrvand N. The effect of prethrombolytic cyclosporine-A injection on clinical outcome of acute anterior ST-elevation myocardial infarction. *Cardiovasc Ther* 2013;31:e34-9.
[PUBMED](#) | [CROSSREF](#)